

# A Biologically Plausible Supervised Learning Method for Spiking Neural Networks Using the Symmetric STDP Rule

Yunzhe Hao<sup>a,b,\*</sup>, Xuhui Huang<sup>a,\*\*</sup>, Meng Dong<sup>a</sup>, Bo Xu<sup>a,b,c</sup>

<sup>a</sup>*Research Center for Brain-inspired Intelligence, Institute of Automation, Chinese Academy of Sciences, 100190 Beijing, China*

<sup>b</sup>*University of Chinese Academy of Sciences, 100049 Beijing, China*

<sup>c</sup>*CAS Center for Excellence in Brain Science and Intelligence Technology, Chinese Academy of Sciences, 100190 Beijing, China*

---

## Abstract

Spiking neural networks (SNNs) possess energy-efficient potential due to event-based computation. However, supervised training of SNNs remains a challenge as spike activities are non-differentiable. Previous SNNs training methods can basically be categorized into two classes, backpropagation-like training methods and plasticity-based learning methods. The former methods are dependent on energy-inefficient real-valued computation and non-local transmission, as also required in artificial neural networks (ANNs), while the latter either be considered biologically implausible or exhibit poor performance. Hence, biologically plausible (bio-plausible) high-performance supervised learning (SL) methods for SNNs remain deficient. In this paper, we proposed a novel bio-plausible SNN model for SL based on the symmetric spike-timing dependent plasticity (sym-STDP) rule found in neuroscience. By combining the sym-STDP rule with bio-plausible synaptic scaling and intrinsic plasticity of the dynamic threshold, our SNN model implemented SL well and achieved good performance in the benchmark recognition task (MNIST). To reveal the underlying mechanism of our SL model, we visualized both layer-based activities and synaptic weights using the t-distributed stochastic neighbor embedding (t-SNE) method after training and

---

\*These two authors contribute equally to this work.

\*\*Corresponding author. E-mail address: xuhui.huang@ia.ac.cn (X. Huang)

found that they were well clustered, thereby demonstrating excellent classification ability. As the learning rules were bio-plausible and based purely on local spike events, our model could be easily applied to neuromorphic hardware for online training and may be helpful for understanding SL information processing at the synaptic level in biological neural systems.

*Keywords:* spiking neural networks, dopamine-modulated spike-timing dependent plasticity, pattern recognition, supervised learning, MNIST dataset, biologically plausibility

---

## 1. Introduction

Due to the emergence of deep learning technology and rapid growth of high-performance computing, artificial neural networks (ANNs) have achieved various breakthroughs in machine learning tasks [1, 2]. However, ANN training is usually energy inefficient as communication among neurons is generally based on real-valued activities and many real-valued weights and error signals need to be transmitted in the basic error backpropagation (BP) training algorithm [3]. Thus, ANNs are highly energy consumptive. Moreover, information processing in human brains is very different to that in ANNs. Neurons in biological systems communicate with each other via spikes or pulses (i.e., event-based communication), with the learning rules for modifying synaptic weights also spike-based, e.g., spike-timing dependent plasticity (STDP) [4, 5, 6], where the weight of a synapse is changed based on spike activities of its pre- and post-synaptic neurons. For these reasons, spiking neural networks (SNNs), which are more biologically appropriate and considered as the third generation of neural network models, have attracted growing interest for exploring their functions in real-world tasks [7, 8].

Unlike that of ANNs, SNN training is highly challenging due to the non-differentiable properties of the spike-type activity. Hence, the development of an efficient training algorithm for SNNs is of considerable importance. Much effort has been expended in the past two decades on this issue [8], with the de-

veloped approaches generally characterized as indirect supervised learning (SL), direct SL, or plasticity-based training [8, 9]. For the indirect SL method, ANNs are first trained and then mapped to equivalent SNNs by different conversion algorithms that transform real-valued computing into spike-based computing [10, 11, 12, 13, 14, 15, 16, 17]; however, this method does not incorporate SNN learning and therefore limits new understanding of the learning nature of SNNs. The direct SL method is based on the BP algorithm [9, 18, 19, 20, 21], e.g., using membrane potentials as continuous variables for calculating errors in BP [18, 21] or using continuous activity function to approximate neuronal spike activity and obtain the differentiable activity for the BP algorithm [9, 20]. However, such research must still perform numerous real-valued computations and communications during the training process, especially the non-local transmission of real-valued synaptic weights and error signals. For plasticity-based training, synaptic plasticity rules (e.g., STDP) are used to extract features for pattern recognition in an unsupervised learning (USL) way [22]. Due to the nature of spontaneous unsupervised clustering of synaptic plasticity, this method requires an additional supervised module for recognition tasks. Three supervised modules have been used in previous studies: a classifier (e.g., support vector machine, SVM) [23], a label statistical method outside the network [22], and an additional supervised layer [24, 25, 26, 27]. In our opinion, a neural network model with biological plausibility must meet the following basic characteristics. Firstly, the single neuron model must integrate temporal inputs and generate pulses or spikes as outputs. Secondly, the computation processes of training and inference must be completely spike-based. Finally, all learning rules must be based on experiments, and should not be violated (obviously contrary to) by experiments or artificially designed. A biologically-plausible model has energy-efficient potential due to event-based computation. The first two supervised modules are bio-implausible due to the need of computation outside the SNNs [23, 22]. The last supervised module has the potential of bio-plausibility, but existing supervised SNN models have either adopted artificially-modified STDP rules [24, 25, 26, 27] or exhibited poor performance [24]. Currently, there-

fore, there is a lack of truly bio-plausible SNN models to accomplish SL with high-performance pattern recognition. Moreover, at the microscopic level, the physiological mechanisms for the modification of synapses have been well uncovered by previous experiments [4, 5]. However, how teacher learning at the macroscopic behavioral level is realized by changes in synapses at the microscopic level, i.e., the mechanism of SL processing in the brain, is still far from clear.

To develop an efficient spike-based SL method for SNNs, we proposed a new bio-plausible SL method for training SNNs based on biological plasticity rules. We introduced the dopamine-modulated STDP (DA-STDP) rule, which was a new type of symmetric STDP (sym-STDP) rule, for pattern recognition. The DA-STDP rule was observed in several different experiments in both hippocampus and prefrontal cortex [28, 29, 30], where the modification of synaptic weight is always incremental if the interval between the pre- and post-synaptic spike activities is within a narrow time-window when dopamine (DA) is present. The differences between the sym- or DA-STDP and classic STDP rules are shown in Figure 1 [4, 28, 30]. While the sym-STDP rule has been used previously [31, 32, 33, 34], this is the first time it has been applied for SL. In our proposed model, a three-layer feedforward SNN was trained by DA-STDP combined with synaptic scaling [35, 36, 37] and dynamic threshold, which were two homeostatic plasticity mechanisms, for stabilizing and specializing the network response under supervised signals. Two different training methods were used in our SNN model, i.e., training two-layer input synaptic weights simultaneously and training the SNN layer-by-layer. We tested our model in the benchmark handwritten digit recognition task (MNIST dataset) and achieved high performance for the two training methods.

## 2. Network architecture and neuronal dynamics

We constructed a three-layer feedforward spiking neural network for SL, which included an input layer, hidden layer, and SL layer (Figure 2). The

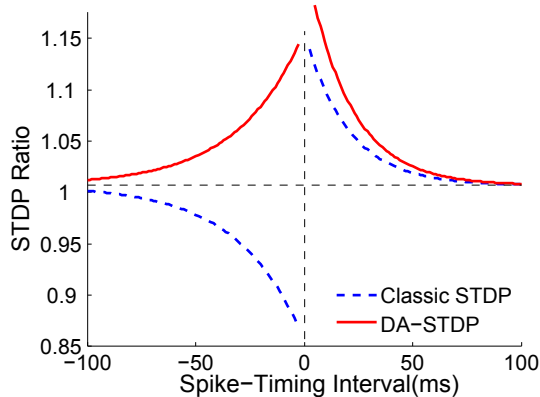


Figure 1: Schematic diagram of the classic STDP [4] and DA-STDP [28, 30].

structure of the first two layers was inspired by the previous USL model of Diehl and Cook [22]. Input patterns were coded as Poisson spike processes with firing rates proportional to the intensities of the corresponding pixels. The Poisson spike trains were then fed to the excitatory neurons in the hidden layer with all-to-all connections. The dark blue shaded area in Figure 2 shows the input connection to a specific neuron. The connection from the excitatory neurons to inhibitory neurons was one-to-one. An inhibitory neuron only received input from the corresponding excitatory neuron at the same position in the map and inhibited the remaining excitatory neurons. All excitatory neurons were fully connected to the neurons in the SL layer. In the supervised layer, neurons fired with two different modes during the training and testing processes. During the SL training period, the label information of the current input pattern was converted to a teacher signal in a one-hot coding scheme by the ten SL neurons. Only one SL neuron was pushed to fire as a Poisson spike process, with the remaining SL neurons maintained in the resting state. In the testing mode, all SL neurons fired according to inputs from the hidden layer.

In our model, the membrane potential ( $V$ ) dynamics of the individual neurons can be described by [22, 38]:

$$\tau \frac{dV}{dt} = (E_{rest} - V) + g_E(E_E - V) + g_I(E_I - V) \quad (1)$$

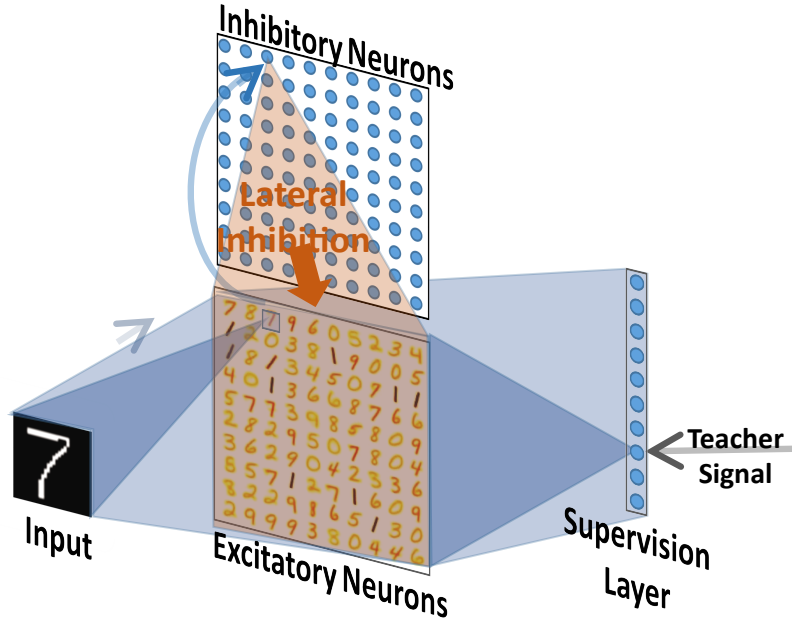


Figure 2: Network structure.

where  $g_E$  and  $g_I$  are the total excitatory conductance and total inhibitory conductance, respectively,  $E_{rest}$  is the resting membrane potential,  $E_E$  and  $E_I$  are the equilibrium potentials of the excitatory and inhibitory synapses, respectively, and  $\tau$  is the time constant of membrane potential damping.

The variables  $g_E$  and  $g_I$  in the leaky integrate-and-fire (LIF) model can be described by the following equations [22, 38]:

$$\tau_{g_E} \frac{dg_E}{dt} = -g_E + \sum_{i=1}^{N_P} \sum_k w_i^{EP} \delta(t - t_i^k) \quad (2)$$

$$\tau_{g_I} \frac{dg_I}{dt} = -g_I + \sum_{i=1}^{N_E} \sum_k w_i^{EI} \delta(t - t_i^k) \quad (3)$$

where  $N_P$  and  $N_E$  are the number of input and excitatory neurons,  $w_i^{EP}$  and  $w_i^{EI}$  are the in-synapse weights of the excitatory neurons and inhibitory neurons,  $t_i^k$  is the  $k$ th spike time from the  $i$ th neuron, and  $\tau_{g_E}$  and  $\tau_{g_I}$  are the time constants of synapse conductance damping.

Synaptic weights were modified according to the two biological plasticity rules, i.e., DA-STDP and synaptic scaling. Dopamine is an important neuro-modulator and plays a critical role in learning and memory processes [39]. Here, inspired by the DA-STDP found in different brain areas, such as the hippocampus and prefrontal cortex [28, 29, 30] (Figure 1), we hypothesized that DA can modulate changes in synaptic weights according to the DA-STDP rule during the SL process. The phenomenological model of DA-STDP can be expressed as [28, 30]:

$$\Delta W = \begin{cases} A_+ \exp(\frac{-\Delta t}{\tau_+}), & \Delta t > 0 \\ A_- \exp(\frac{\Delta t}{\tau_-}), & \Delta t < 0 \end{cases} \quad (4)$$

where  $\Delta W$  refers to the weights increment,  $\Delta t$  is the time difference between the pre- and post-synaptic spikes,  $\tau_+$  and  $\tau_-$  are the time constants of positive and negative phases for  $\Delta t$ , respectively, and  $A_+$  and  $A_-$  are the learning rates,  $A_+, A_- \geq 0$ .

Because DA-STDP can only increase synapse strength at any time, the synaptic scaling plasticity rule was used to introduce a competition mechanism among all input synapses (in-synapses) of a neuron in the hidden layer (only for excitatory neurons) and SL layer. Synaptic scaling is a homeostatic plasticity mechanism observed in many experiments [40, 35, 41], especially in visual systems [42, 43, 44] and the neocortex [36]. Here, synaptic scaling was conducted after the pattern was trained and adjusted according to the following equation [22]:

$$w_{\text{new}} = w_{\text{old}} \frac{\alpha N_{\text{in}}}{\sum w_{\text{old}}} \quad (5)$$

where  $N_{\text{in}}$  is the number of all in-synapses of a neuron and  $\alpha$  is the scaling factor with  $\alpha \in (0, 1)$ . The sum iterates over all incoming weights of a neuron. In our model, the dynamic threshold homeostatic plasticity mechanism was also adopted. The dynamic threshold is the intrinsic plasticity of a neuron, and is found in different neural systems [45, 46, 47, 40, 48]. Here, it was introduced to generate a specific response to a class of input patterns for each excitatory neu-

ron in the hidden layer [47, 40, 22], otherwise a single neuron will dominate the response pattern due to its enlarged in-synaptic weights and lateral inhibition. That is, the potential threshold of a neuron will be increased with a certain amplitude after the neuron spikes, which can be described as:

$$V_{\text{thres}} = V_{\theta} + \theta - \theta_{\text{initial}} \quad (6)$$

$$\frac{d\theta}{dt} = -\frac{\theta}{\tau_{\theta}} + \Delta_{\theta} \sum_k \delta(t - t_k) \quad (7)$$

where  $\Delta_{\theta}$  is a function of current  $\theta$  and set to  $\theta_+ * \frac{\theta_{\text{initial}}}{|2\theta - \theta_{\text{initial}}|}$  to avoid excessive growth.

### 3. Recognition performance for the MNIST task

Our SNN model was trained on the MNIST dataset (training set: 60000 samples; test dataset: 10000 samples) (<http://yann.lecun.com/exdb/mnist/>) using two training methods, i.e., simultaneous and layer-by-layer training. For simultaneous training, the in-synapses of the hidden layer and SL layer were updated simultaneously during the training process, whereas for layer-by-layer training, the hidden layer was trained first followed by the SL layer, then the SL layer was trained with all in-synaptic weights of the hidden layer fixed. There was no preprocessing of the data and we used a SNN simulator (GeNN) [49] to simulate all experiments. For the model parameters, we set the simulation time step to 0.5 ms and the presentation time of an input sample to the network to 350 ms followed by a resting period of 150 ms. Other neuron parameters were as follows:  $\tau = 100$ ,  $E_{rest} = -65\text{mV}$ ,  $E_E = 0\text{mV}$ ,  $E_I = -100\text{mV}$ ,  $\tau_{g_E} = 1$ ,  $\tau_{g_I} = 1$ ,  $\tau_+ = 20$ ,  $\tau_- = 20$ ,  $\alpha = 0.1$ ,  $V_{\theta} = -72\text{mV}$ ,  $\theta_{\text{initial}} = 20\text{mV}$ . Both  $\tau_{\theta}$  and  $\theta_+$  were set according to network size. The in-synaptic and out-synaptic weights of the excitatory neurons in the hidden layer were set to the ranges of  $[0, 1]$  and  $[0, 8]$ , respectively. All initial weights were set to corresponding maximum weights multiplied by uniform distributed values in the range  $[0, 0.3]$ . For the learning rates of STDP,  $A_+$  and  $A_-$  were set to the same value, which equaled 0.001 and 0.002 for in-synaptic and out-synaptic weights of the hidden



layer, respectively. The firing rates of the input neurons were proportional to the intensity of the pixels of the MNIST images [22]. We also set maximum rates to 63.75 Hz after dividing the maximum pixel intensity of 255 by 4. When less than five spikes were found in the excitatory neurons of the hidden layer during 350 ms, the maximum input firing rates were increased by 32 Hz. The firing rates of the SL neurons were 200 Hz or 0 Hz according to the one-hot code in the SL training period.

To demonstrate the power of the proposed SL method for different network sizes, we compared the results of our learning algorithm to the ‘Label Statistics’ learning algorithm used in previous research [22]. ‘Label Statistics’ method has two phases named ‘label’ and ‘statistics’. Specifically, after the unsupervised training using STDP, the excitatory neuron in the hidden layer has a special receptive field, which makes various degrees of response to one sample. Then the neuron obtains the label of the strongest response sample. It is the ‘label’ phase. In the testing, we get the all class votes using the ‘statistics’ method, i.e., to accumulate all of the same label neuron spike counts as the likelihood of this class. Finally, the label of most votes is the predicted label.

We trained the model with different epochs of the training dataset for different network sizes (3, 5, 7, 10, and 20 epochs for  $N_e = 100, 400, 1600, 6400,$  and 10000, respectively). During the training process, the network performances for each of 10000 samples were estimated by the test dataset. Taking networks with sizes  $N_e = 400$  and 6400 as examples, classifying accuracies converged quickly under the two training methods (Figure 3). Figure 4 shows very high consistency between the desired (label) and inferred (real) outputs in the SL layer.

The results for the different learning methods are summarized in Table 1. Our SL model outperformed the ‘Label Statistics’ method for small-sized networks ( $N \leq 1600$ ), except for the re-training case with  $N_e = 100$ , and its performance was only slightly lower than the ‘Label Statistics’ method for large-sized networks ( $N_e = 6400$  and 10000). The best performance of our SL model (96.56%) was achieved in the largest network under Layer-by-Layer training.

These results indicated that a SNN equipped with biologically realistic plasticity rules can achieve good SL by pure spike-based computation.

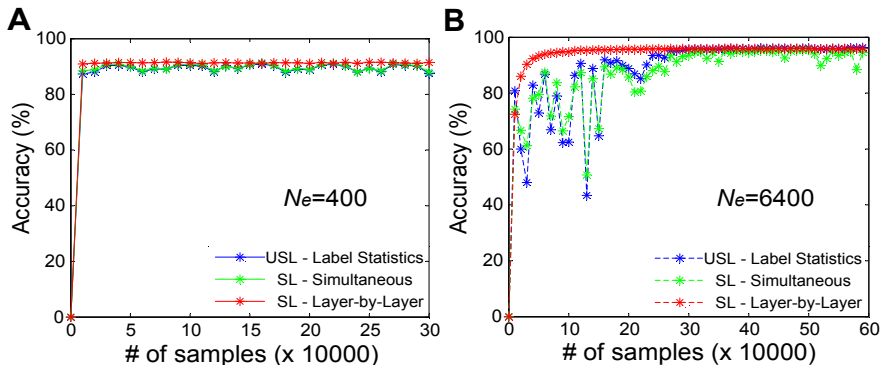


Figure 3: Convergence property of networks with sizes  $N_e = 400$  (A) and  $6400$  (B). The ‘Layer-by-Layer’ curve in each figure represents SL performance under layer-by-layer training using STDP to train in-synaptic weights of the hidden layer in unsupervised style and then train out-synaptic weights in the supervised style.

#### 4. Visualization of the model clustering ability

To demonstrate the underlying mechanisms of our SL model in pattern recognition tasks, we adopted the popular dimension-reduction method t-distributed Stochastic Neighbor Embedding (t-SNE) [50] to reveal the models clustering ability. The t-SNE is a nonlinear dimensionality reduction method and widely used for visualizing the high-dimensional data in a low-dimensional space of two or three dimensions. We first visualized the original digit patterns (Figure 5A), spike activities of the hidden layer (Figure 5B), and spike activities of the SL layer (Figure 5C) for all samples in the test dataset. The separability of the output information of the three layers in our model increased from the input to SL layer, which indicated that the SL layer served as a good classifier after training. To demonstrate why our SL method achieved effective clustering for the hidden layer outputs, we also adopted the t-SNE method to reduce the dimensions of the out-synaptic weights of the excitatory neurons. As shown in Figure 6, the clustering of the out-synaptic weights of the excitatory neurons was

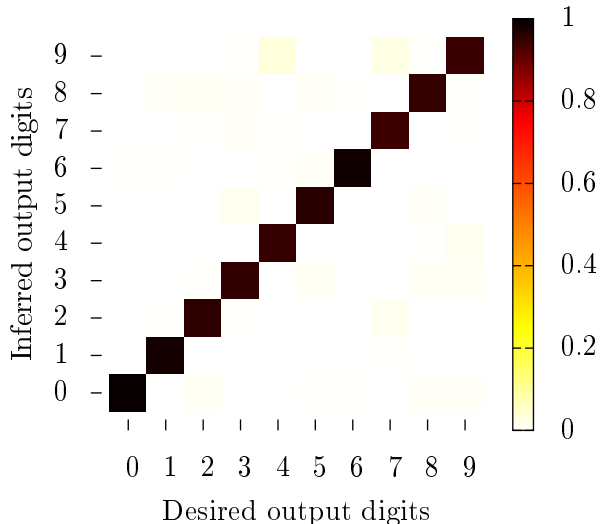


Figure 4: Confusion matrix of test dataset results in the SL layer for the network with size  $N_e = 6400$ . The darker pixel indicates stronger consistency between desired (label) and inferred (real) outputs. Data were obtained for re-trained SL, as shown in Figure 3B .

highly consistent with the clustering of their label information using the ‘Label Statistics’ method. This explains why our SL method achieved comparatively good performance as the ‘Label Statistics’ method for the classification task, although our model does not require ‘Label Statistics’ computation outside the network to calculate the most likely representation of a hidden neuron [22] and realizes the SL process based solely on computation within the network.

## 5. Comparison to other SNN models

Current SNN models for pattern recognition can be generally categorized into three classes: that is, indirect training [10, 11, 12, 13, 14, 15, 16, 17], direct SL training with BP [9, 24, 18, 19, 20, 21, 51], and plasticity-based unsupervised training with supervised modules [52, 22, 23]. Table 2 summaries several previous SNN models trained and tested on full training and testing sets of the MNIST dataset. In our model, we used bio-plausible neuroplasticity rules (i.e.,

Network Size ( $N_e$ )		100	400	1600	6400	10000
Simultaneous Training	Label Stat.	83.11%	90.89%	91.18%	96.29%	96.81%
	SL Method	83.11%	91.31%	91.33%	95.81%	95.82%
Layer-by-layer Training	Label Stat.	83.22%	91.11%	91.91%	96.34%	96.97%
	SL Method	83.20%	91.55%	92.33%	96.17%	96.56%

Table 1: Performance for different sized networks with different training methods. ‘Label Stat.’ represents classification by the ‘Label Statistics’ method in the hidden layer, for details please refer to [22]. Each pair of accuracies under the ‘Label Statistics’ method and SL method are measured at the same time in the training process. The highest accuracy in each training trial is reported here. For network size  $N_e = 100, 400, 1600, 6400$  and  $10000$ ,  $\tau_\theta = 6 \times 10^6, 6 \times 10^6, 8 \times 10^6, 2 \times 10^7$  and  $2 \times 10^7$ ;  $\theta_+ = 0.7, 0.7, 0.7, 0.5$  and  $0.5$ , respectively.

sym-STDP and synaptic scaling) and local spike-based computation to accomplish SL, without the need of backpropagation or error computation. Thus, the proposed method provides a novel model framework to achieve efficient SL in SNNs.

**Comparison to SNN models trained using BP.** In previous studies with indirect training, ANNs were trained using the BP algorithm based on activity rates and transformed to corresponding equivalent SNNs based on firing rates. Although their performances were very good, they ignored the temporal evolution of SNNs and spike-based learning processes. Thus, indirect training provides very little enlightenment on how SNNs learn and encode different features of inputs. For other studies using direct SL training, most adopted the BP algorithm and calculated errors based on continuous variables—membrane potentials (voltage), currents, or activity rates to approximate spike activities and realize SL [9, 18, 19, 20, 21, 51]. For example, Zhang et al. proposed a voltage-driven plasticity-centric SNN for SL [21], with four learning stages required for training, i.e., equilibrium learning and voltage-based STDP for USL and BP for the final SL. However, this model is highly dissimilar to biological neuronal systems and is energy inefficient. Lee et al. pre-trained multi-layer

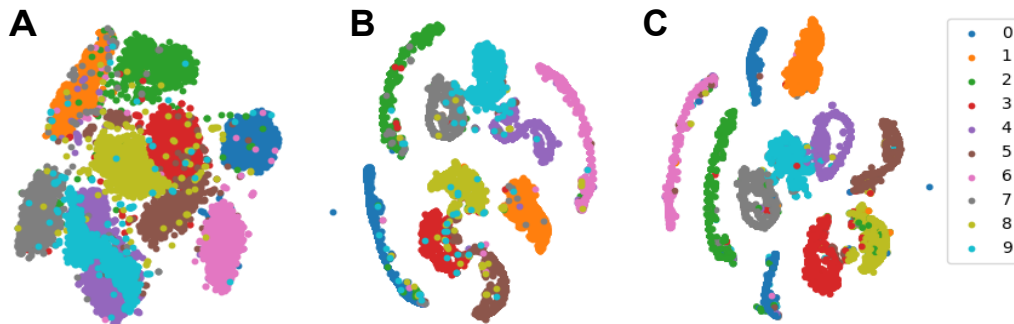


Figure 5: Visualization of the original digit patterns (A), spike activities of the hidden layer (B), and spike activities of the SL layer (C) for the MNIST test dataset using the t-SNE method. Each dot represents a digit sample and is colored by its corresponding label information. Activities were obtained by testing the performance of the final synaptic weights in the case of the re-trained SL for  $N_e = 6400$  (shown in Figure 3).

SNN systems by STDP in an USL way for optimal initial weights and then used current-based BP to re-train all-layer weights in a supervised way [51]. However, this model is bio-implausible, requires non-local computation, and is also energy inefficient.

**Comparison to STDP-based models without BP.** Several studies have also proposed STDP-based training methods without BP. These previous models adopted STDP-like plasticity rules for USL and required a special supervised module for SL, e.g., a classifier (SVM) [23], artificial label statistics outside network [52, 22], or an additional supervised layer [24, 25, 26, 27]. However, the first two supervised modules are bio-implausible because their computing modules are outside the SNNs, resulting in the SNNs having no direct relationship with SL [52, 22, 23]. For example, Beyeler et al. adopted a calcium concentration-based STDP for SL [24], although it was inspired by experiments, which showed considerably poorer performance than that of our model. Hu et al. used an artificially-modified STDP with a special temporal learning phase for SL [25]; however, their STDP rule was artificially designed and its internal mechanism was not well explained. Shrestha et al. also adopted a specially-modified STDP rule with exponential weight change and extended depression

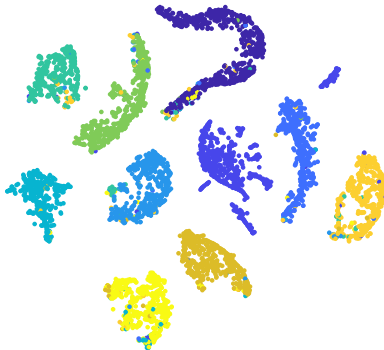


Figure 6: Visualization of the clustering ability of out-synapses of excitatory neurons in the hidden layer ( $N_e = 6400$ ) to the SL layer using the t-SNE method. Each dot represents an excitatory neuron in the hidden layer and is colored by its label using the ‘Label Statistics’ method. The clustering of the out-synaptic weights of the excitatory neurons is highly consistent with the clustering of their labels. The synaptic weights used here were from the case in Figure 5.

window for SL in a SNN, with a similar supervised module as ours, but performance was relatively poor (less than 90% ) [26]. Mozafari et al. used a mixed classic STDP and anti-STDP rule to generate reward-modulated STDP with a remote supervised spike for SL, but they were not able to provide biological evidence to explain this type of learning [27].

**Detail comparison to the STDP-based SNN model by Diehl and Cook.** Our model was inspired by the previous STDP-based SNN method proposed by Diehl and Cook [22]. In their two-layer SNN, STDP is used to extract features by USL and an additional computing module outside the SNN is used for label statistics in the training process and classification in the testing process. The additional module first calculates the most likely representation of a neuron for a special class of input patterns, labels the neuron to the class during the training process, and uses the maximum mean firing rates among all classes of labeled neurons for inference in the test process. In our model, however, we achieved the same algebraic computation and reasoning using an additional layer of spiking neurons instead of the outside-network computations, which made a great progress of STDP-based SNN model for SL due to the completely

spike-based computation. Moreover, there were two other improvements in our model compared to that of Diehl and Cook [22]. The first improvement was the novel sym-STDP rule rooted in DA-STDP, with DA-STDP able to give a potential explanation for the SL processes occurring in the brain. That is, we assumed that DA may be involved in the SL process and that local synaptic plasticity could be changed to sym-STDP during the whole training process. With the aid of the forced firing of a supervised neuron by the incoming teacher signal, sym-STDP could establish the relationship between the input and its teacher information after sufficient training. The second improvement was the new dynamic threshold rule, in which the multiplicative learning rate was replaced by the fixed learning rate of the threshold increment, which significantly improved performance.

It should be noted that, there were also a few SNN training models that can do classification tasks in other ways, but their recognition performance was not very good [53, 54]. For example, recently, Xu et al. constructed a novel convolutional spiking neural network (CSNN) model by using the tempotron as the classifier, and attempted to take advantage of both convolutional structure and SNN’s temporal coding ability [55]. But their model’s performance was not good and only reached the maximal accuracy of 88% on a subset of MNIST dataset (Training samples: 500; Test samples: 100) when the network size equalled 1200, in contrast with the accuracy of 91.55% in our case with  $N_e = 400$  on the full MNIST dataset. This reveals that our model could also work very well under the small network size constraint.

Thus, for the above reasons, our proposed sym-STDP based SNN model could solve the lack of bio-plausible and high-performance SNN methods for spike-based SL.

## 6. Discussion

A neural network model with biological plausibility must meet three basic characteristics, i.e., the ability to integrate temporal input and generate spike

Network model	Learning method	Training type	(Un-)Supervised	Accuracy
<b>In-direct training</b>				
Deep LIF SNN [11]	BP-ANN conversion	Rate-based	Supervised	98.37%
CSNN[12]	BP-ANN conversion	Rate-based	Supervised	99.1%
Chip-based SNN [13]	BP-ANN conversion	Rate-based	Supervised	99.42%
SDRN[17]	BP-ANN conversion	Rate-based	Supervised	99.59%
<b>Direct training</b>				
BP-STDP SNN[20]	BP-STDP	Rate-based	Supervised	96.6%
Deep LIF-BA SNN [19]	Broadcast Alignment	Rate-based	Supervised	97.05%
STBP SNN[9]	Spatio-Temporal BP	Rate-based	Supervised	98.89%
VDPC SNN [21]	Equilibrium learning + STDP	Voltage-based	Supervised	98.52%
Deep SNN[18]	BP	Voltage-based	Supervised	98.88%
DCSNN[51]	STDP + BP	Spike-based & Current-based	Supervised	99.28%
Two-layer SNN[52]	Rectangular STDP	Spike-based	Unsupervised	93.5%
Two-layer SNN [22]	Exponential STDP	Spike-based	Unsupervised	95.0%
SDNN[23]	STDP + SVM	Spike-based	Unsupervised	98.4%
Three-layer SNN[26]	Specially modified STDP	Spike-based	Supervised	89.7%
MLHN[24]	STDP with Calcium variable	Spike-based	Supervised	91.6%
Bidirectional SNN[25]	Specially modified STDP	Spike-based	Supervised	96.8%
DCSNN[27]	STDP + R-STDP	Spike-based	Supervised	97.2%
Sym-STDP SNN ( <b>Ours</b> )	Sym-STDP (DA-STDP)	Spike-based	Supervised	96.56%

Table 2: Comparison of classification performance of our SNN model to the others on the MNIST task. All models reported here were trained based on the full training dataset and tested by the full testing dataset. LIF: Leaky integrate-and-fire; BP: Backpropagation; CSNN: Convolutional spiking neural network; SDRN: Spiking deep residual network; MLHN: Multi-layer hierarchical network; STBP: Spatio-temporal backpropagation; VDPC: Voltage-driven plasticity-centric; BA: Broadcast alignment; SDNN: Spiking deep neural network; SVM: Support vector machine; R-STDP: Reward-modulated STDP.

output, spike-based computation for training and inference, and all learning rules rooted in biological experiments. Here, we used the LIF neuron model, with all learning rules (e.g., sym-STDP, synaptic scaling, and dynamic threshold) observed in all experiments and computation based on spikes. Thus, the proposed SNN model meets all the above requirements and is a true biologically plausible neural network model.

However, how did our model obtain good pattern recognition performance? This was mainly because the three learning rules worked synergistically to



achieve feature extraction and expected relationship between input and output. The sym-STDP rule demonstrated a considerable advantage by extracting the relationship of spike events regardless of the temporal order in two connected neurons, with synaptic scaling able to stabilize total in-synaptic weights and create weight competition among in-synapses of a neuron to ensure that the suitable group of synapses became strong. Furthermore, the dynamic threshold mechanism compelled a neuron to fire for matched patterns but rarely fire for unmatched ones, which generated neuron selectivity to a special class of patterns. By combining the three bio-plausible plasticity rules, our SNN model established a strong relationship between the input signal and supervised signal after sufficient training, ensuring effective SL implementation and good performance in the benchmark pattern recognition task (MNIST). The proposed model also obtained good performance when training two layers synchronously, whereas many previous SNN models can only be trained using the layer-by-layer or multi-phase/multi-step methods [23, 18, 19, 21, 25].

In our SNN model, DA was found to be a key factor for achieving SL. Dopamine plays a critical role in different learning processes and can serve as a reward signal for reinforcement learning [56, 57, 58, 59]. A special form of dopamine-modulated STDP, different with the symmetric one used here, had been applied to realize reinforcement learning in SNNs [60], but there is no direct experimental evidence for this kind of STDP rule. Here, we assumed that DA may also be involved in the SL process, with the symmetric DA-STDP rule found in experiments to modify synaptic weights during SL. Our work further indicated the potentially diverse functions of DA in regulating neural networks for information processing.

It is worth noting that the sym-STDP rule is a spiking version of the original Hebbian rule, that is, ‘cells that fire together wire together’, and a rate-based neural network with the Hebbian rule, synaptic scaling, and dynamic bias could be expected to have similar classification ability as our model. However, the performance of the rate model may not be as high as that reported here. Further exploration is needed using the simplified rate model with the original Hebbian

rule.

As the plasticity rules we used were purely based on local spike events, in contrast with the BP method, our model not only has the potential to be applied to other machine learning tasks under the SL framework but may also be suitable for online learning on programmable neuromorphic chips. Moreover, our hypothesis about the function of DA in SL processing could serve as a potential mechanism for the synaptic information processing of SL in the brain, which will need to be verified in future experiments.

### **Acknowledgments**

This work was supported by the Natural Science Foundation of China (Grant No. 11505283), the Strategic Priority Research Program of the Chinese Academy of Sciences (Grant No. XDBS01070000), and the Independent Deployment Project of CAS Center for Excellence in Brain Science and Intelligent Technology (Grant No. CEBSIT2017-02). We also gratefully acknowledge the support of the NVIDIA Corporation with the donation of the Titan X Pascal GPU used for this research.

### **References**

- [1] Y. LeCun, Y. Bengio, G. Hinton, Deep learning, *Nature* 521 (7553) (2015) 436–444.
- [2] J. Schmidhuber, Deep learning in neural networks: An overview, *Neural Networks* 61 (2015) 85–117.
- [3] D. E. Rumelhart, G. E. Hinton, R. J. Williams, et al., Learning representations by back-propagating errors, *Cognitive modeling* 5 (3) (1988) 1.
- [4] G.-q. Bi, M.-m. Poo, Synaptic modifications in cultured hippocampal neurons: dependence on spike timing, synaptic strength, and postsynaptic cell type, *J. Neurosci.* 18 (24) (1998) 10464–10472.

- [5] N. Caporale, Y. Dan, Spike timing-dependent plasticity : A hebbian learning rule, *Annu . Rev . Neurosci* 31 (2008) 25–46.
- [6] S. Song, K. D. Miller, L. F. Abbott, Competitive hebbian learning through spike-timing-dependent synaptic plasticity, *Nature neuroscience* 3 (9) (2000) 919.
- [7] W. Maass, H. Markram, On the computational power of circuits of spiking neurons, *J. Comput. Syst. Sci.* 69 (4) (2004) 593–616.
- [8] A. Tavanaei, M. Ghodrati, S. R. Kheradpisheh, T. Masquelier, A. S. Maida, Deep learning in spiking neural networks, arXiv preprint arXiv:1804.08150.
- [9] Y. Wu, L. Deng, G. Li, J. Zhu, L. Shi, Spatio-temporal backpropagation for training high-performance spiking neural networks, arXiv preprint arXiv:1706.02609.
- [10] Y. Cao, Y. Chen, D. Khosla, Spiking deep convolutional neural networks for energy-efficient object recognition, *Int. J. Comput. Vision* 113 (1) (2015) 54–66.
- [11] E. Hunsberger, C. Eliasmith, Spiking deep networks with lif neurons, arXiv preprint arXiv:1510.08829.
- [12] P. U. Diehl, D. Neil, J. Binas, M. Cook, S.-C. Liu, M. Pfeiffer, Fast-classifying, high-accuracy spiking deep networks through weight and threshold balancing, in: *IJCNN, IEEE*, 2015, pp. 1–8.
- [13] S. K. Esser, R. Appuswamy, P. A. Merolla, J. V. Arthur, D. S. Modha, Backpropagation for energy-efficient neuromorphic computing, *NIPS* (2015) 1117–1125.
- [14] P. U. Diehl, G. Zarrella, A. Cassidy, B. U. Pedroni, E. Neftci, Conversion of artificial recurrent neural networks to spiking neural networks for low-power neuromorphic hardware, in: *ICRC, IEEE*, 2016, pp. 1–8.

- [15] D. Neil, S.-C. Liu, Effective sensor fusion with event-based sensors and deep network architectures, in: ISCAS, IEEE, 2016, pp. 2282–2285.
- [16] S. K. Esser, P. A. Merolla, J. V. Arthur, A. S. Cassidy, R. Appuswamy, A. Andreopoulos, D. J. Berg, J. L. McKinstry, T. Melano, D. R, et al., Convolutional networks for fast, energy-efficient neuromorphic computing, *Proc. Natl. Acad. Sci. U. S. A.* 113 (41) (2016) 11441–11446.
- [17] Y. Hu, H. Tang, Y. Wang, G. Pan, Spiking deep residual network, arXiv preprint arXiv:1805.01352.
- [18] J. H. Lee, T. Delbruck, M. Pfeiffer, Training deep spiking neural networks using backpropagation, *Front. Neurosci.* 10.
- [19] A. Samadi, T. P. Lillicrap, D. B. Tweed, Deep learning with dynamic spiking neurons and fixed feedback weights, *Neural Comput.* 29 (3) (2017) 578–602.
- [20] A. Tavanaei, A. S. Maida, Bp-stdp: Approximating backpropagation using spike timing dependent plasticity, arXiv preprint arXiv:1711.04214.
- [21] T. Zhang, Y. Zeng, D. Zhao, M. Shi, A plasticity-centric approach to train the non-differential spiking neural networks, in: AAAI, 2018.
- [22] P. U. Diehl, M. Cook, Unsupervised learning of digit recognition using spike-timing-dependent plasticity, *Front. Comput. Neurosci.* 9.
- [23] S. R. Kheradpisheh, M. Ganjtabesh, S. J. Thorpe, T. Masquelier, Stdp-based spiking deep convolutional neural networks for object recognition, *Neural Networks* 99 (2018) 56–67.
- [24] M. Beyeler, N. D. Dutt, J. L. Krichmar, Categorization and decision-making in a neurobiologically plausible spiking network using a stdp-like learning rule, *Neural Networks* 48 (10) (2013) 109–124.
- [25] Z. Hu, T. Wang, X. Hu, An stdp-based supervised learning algorithm for spiking neural networks, in: ICONIP, Springer, 2017, pp. 92–100.

- [26] A. Shrestha, K. Ahmed, Y. Wang, Q. Qiu, Stable spike-timing dependent plasticity rule for multilayer unsupervised and supervised learning, in: Neural Networks (IJCNN), 2017 International Joint Conference on, IEEE, 2017, pp. 1999–2006.
- [27] M. Mozafari, M. Ganjtabesh, A. Nowzari-Dalini, S. J. Thorpe, T. Masquelier, Combining stdp and reward-modulated stdp in deep convolutional spiking neural networks for digit recognition, arXiv preprint arXiv:1804.00227.
- [28] J. C. Zhang, P. M. Lau, G. Q. Bi, C. F. Stevens, Gain in sensitivity and loss in temporal contrast of stdp by dopaminergic modulation at hippocampal synapses, *Proc. Natl. Acad. Sci. U. S. A.* 106 (31) (2009) 13028–13033.
- [29] H. Ruan, T. Saur, W.-D. Yao, Dopamine-enabled anti-Hebbian timing-dependent plasticity in prefrontal circuitry, *Front. Neural Circuit.* 8 (April) (2014) 1–12.
- [30] Z. Brzosko, W. Schultz, O. Paulsen, Retroactive modulation of spike timing-dependent plasticity by dopamine, *Elife* 4.
- [31] N. Masuda, H. Kori, Formation of feedforward networks and frequency synchrony by spike-timing-dependent plasticity, *Journal of computational neuroscience* 22 (3) (2007) 327–345.
- [32] H. Tanaka, T. Morie, K. Aihara, A cmos spiking neural network circuit with symmetric/asymmetric stdp function, *IEICE transactions on fundamentals of electronics, communications and computer sciences* 92 (7) (2009) 1690–1698.
- [33] T. Serrano-Gotarredona, T. Masquelier, T. Prodromakis, G. Indiveri, B. Linares-Barranco, Stdp and stdp variations with memristors for spiking neuromorphic learning systems, *Front. Neurosci.* 7 (2013) 2.

- [34] R. K. Mishra, S. Kim, S. J. Guzman, P. Jonas, Symmetric spike timing-dependent plasticity at ca3–ca3 synapses optimizes storage and recall in autoassociative networks, *Nature communications* 7 (2016) 11552.
- [35] G. G. Turrigiano, The self-tuning neuron: Synaptic scaling of excitatory synapses, *Cell* 135 (3) (2008) 422–435.
- [36] G. G. Turrigiano, K. R. Leslie, N. S. Desai, L. C. Rutherford, S. B. Nelson, Activity-dependent scaling of quantal amplitude in neocortical neurons, *Nature* 391 (6670) (1998) 892.
- [37] F. Effenberger, J. Jost, A. Levina, Self-organization in balanced state networks by stdp and homeostatic plasticity, *PLoS Comput. Biol.* 11 (9).
- [38] T. P. Vogels, H. Sprekeler, F. Zenke, C. Clopath, W. Gerstner, Inhibitory plasticity balances excitation and inhibition in sensory pathways and memory networks, *Science* 334 (6062) (2011) 1569–1573.
- [39] N. X. Tritsch, B. L. Sabatini, Dopaminergic modulation of synaptic transmission in cortex and striatum, *Neuron* 76 (1) (2012) 33–50.
- [40] K. Pozo, Y. Goda, Unraveling mechanisms of homeostatic synaptic plasticity, *Neuron* 66 (3) (2010) 337–351.
- [41] G. W. Davis, Homeostatic control of neural activity: from phenomenology to molecular design, *Annu. Rev. Neurosci.* 29 (2006) 307–323.
- [42] A. Maffei, G. G. Turrigiano, Multiple modes of network homeostasis in visual cortical layer 2/3, *Journal of Neuroscience* 28 (17) (2008) 4377–4384.
- [43] T. Keck, G. B. Keller, R. I. Jacobsen, U. T. Eysel, T. Bonhoeffer, M. Hübener, Synaptic scaling and homeostatic plasticity in the mouse visual cortex in vivo, *Neuron* 80 (2) (2013) 327–334.
- [44] K. B. Hengen, M. E. Lambo, S. D. Van Hooser, D. B. Katz, G. G. Turrigiano, Firing rate homeostasis in visual cortex of freely behaving rodents, *Neuron* 80 (2) (2013) 335–342.

- [45] L. C. Yeung, H. Z. Shouval, B. S. Blais, L. N. Cooper, Synaptic homeostasis and input selectivity follow from a calcium-dependent plasticity model, *Proceedings of the National Academy of Sciences* 101 (41) (2004) 14943–14948.
- [46] Q.-Q. Sun, Experience-dependent intrinsic plasticity in interneurons of barrel cortex layer iv, *Journal of Neurophysiology* 102 (5) (2009) 2955–2973.
- [47] W. Zhang, D. J. Linden, The other side of the engram: experience-driven changes in neuronal intrinsic excitability, *Nature Reviews Neuroscience* 4 (11) (2003) 885.
- [48] L. N. Cooper, M. F. Bear, The bcm theory of synapse modification at 30: interaction of theory with experiment, *Nature Reviews Neuroscience* 13 (11) (2012) 798.
- [49] E. Yavuz, J. Turner, T. Nowotny, Genn: a code generation framework for accelerated brain simulations, *Scientific reports* 6 (2016) 18854.
- [50] L. v. d. Maaten, G. Hinton, Visualizing data using t-sne, *J. Mach. Learn. Res.* 9 (Nov) (2008) 2579–2605.
- [51] C. Lee, P. Panda, G. Srinivasan, K. Roy, Training deep spiking convolutional neural networks with stdp-based unsupervised pre-training followed by supervised fine-tuning, *Frontiers in Neuroscience* 12 (2018) 435.
- [52] D. Querlioz, O. Bichler, P. Dollfus, C. Gamrat, Immunity to device variations in a spiking neural network with memristive nanodevices, *IEEE Trans. Nanotechnol.* 12 (3) (2013) 288–295.
- [53] Z. Lin, D. Ma, J. Meng, L. Chen, Relative ordering learning in spiking neural network for pattern recognition, *Neurocomputing* 275 (2018) 94–106.
- [54] I. Sporea, A. Grüning, Supervised learning in multilayer spiking neural networks, *Neural computation* 25 (2) (2013) 473–509.

- [55] Q. Xu, Y. Qi, H. Yu, J. Shen, H. Tang, G. Pan, Csn: An augmented spiking based framework with perceptron-inception., in: IJCAI, 2018, pp. 1646–1652.
- [56] P. W. Glimcher, Understanding dopamine and reinforcement learning: the dopamine reward prediction error hypothesis, *Proceedings of the National Academy of Sciences* 108 (Supplement 3) (2011) 15647–15654.
- [57] C. B. Holroyd, M. G. Coles, The neural basis of human error processing: reinforcement learning, dopamine, and the error-related negativity., *Psychological review* 109 (4) (2002) 679.
- [58] R. A. Wise, Dopamine, learning and motivation, *Nature reviews neuroscience* 5 (6) (2004) 483.
- [59] P. Dayan, B. W. Balleine, Reward, motivation, and reinforcement learning, *Neuron* 36 (2) (2002) 285–298.
- [60] E. M. Izhikevich, Solving the distal reward problem through linkage of stdp and dopamine signaling, *Cereb. Cortex* 17 (10) (2007) 2443–2452.